

## Polymer crystallization: fold surface free energy determination by different thermal analysis techniques<sup>☆</sup>

A. Celli<sup>a,\*</sup>, E.D. Zanotto<sup>b</sup>

<sup>a</sup> *Himont (Montedison Group), "Giulio Natta" Research Center, 44100 Ferrara, Italy*

<sup>b</sup> *Department of Materials Engineering, Federal University of São Carlos,  
13565-905 São Carlos - SP, Brazil*

Received 16 September 1994; accepted 13 March 1995

---

### Abstract

Three different thermal analysis techniques (DSC, and hot-stage optical microscopy equipped with a photodiode to measure light depolarization or a video system to measure spherulitic growth) were used to study polymer crystallization. The fold surface free energy ( $\sigma_e$ ) values from different analytical methods on five polymers are compared. The overall crystallization data always yield  $\sigma_e$  values 15–50% higher than those obtained from the more direct method of measuring growth rate.

*Keywords:* Crystallization; DSC; Microscopy; Polymer

---

### 1. Introduction

The determination of the fold and lateral surface free energies  $\sigma$  and  $\sigma_e$  is very significant in the understanding of polymer crystallization. If one accepts the theory that describes polymer crystallization as a phenomenon of secondary surface nucleation [1],  $\sigma$  and  $\sigma_e$  are the key parameters controlling both crystal nucleation and crystal growth rates.

The difficulty in determining  $\sigma_e$  experimentally results from the small size and the thinness of polymer crystals.

---

\* Corresponding author.

<sup>☆</sup> Presented at the 6th European Symposium on Thermal Analysis and Calorimetry, Grado, Italy 11–16 September 1994.

A thermodynamic approach is based on the approximate expression [1]

$$T_m = T_m^{\circ} [1 - 2\sigma_e / (\Delta h_m) l] \quad (1)$$

where  $T_m$  and  $T_m^{\circ}$  are the melting temperature of a lamella of thickness  $l$  and the equilibrium melting temperatures respectively,  $\Delta h_m$  is the bulk free energy of melting, and  $l$  the thin dimension of the crystal. Thus by plotting  $T_m$  versus  $1/l$  one finds the slope is  $(-2\sigma_e T_m^{\circ} / \Delta h_m)$  and the intercept ( $T_m^{\circ}$ ). Then, if  $\Delta h_m$  is known,  $\sigma_e$  can be determined. In this case it is necessary to know the thickness  $l$ , whose values can be obtained by sophisticated techniques (SAXS, for example).

The kinetic approach, however, uses thermal analysis to follow the crystallization process under isothermal conditions. This method is widely used and an extensive bibliography can be found in the literature. However, a general critical view on the results obtained from the kinetic approach is not yet available.

The objective of this paper is to compare the different thermal analysis techniques and the different analytical methods used in the literature to determine the fold surface free energy value. This work has been performed on three polymers in order to obtain a general conclusion. Literature data concerning two additional polymers are also compared and critically discussed.

## 2. Materials and experimental techniques

Two polypropylene homopolymers (PP), produced by Himont (Italy), and a poly(ethylene terephthalate) (PET) sample, produced by Enichem Polimeri (Italy), were used in the experimental part of this work.

The first PP sample, specimen A, is characterized by:  $[\eta] = 3.48 \text{ dl g}^{-1}$ ,  $M_w = 947\,000$ ,  $MWD = 8.7$ , and isotactic index = 96.5%, measured by NMR triades. The PP sample B is characterized by:  $[\eta] = 0.66 \text{ dl g}^{-1}$ ,  $M_w = 129\,000$ ,  $MWD = 11$ , and isotactic index = 97%. The specimens were stabilized by adding a mixture of Irganox 1010 and Irgafos 168 in a 1:2 ratio (1600 ppm by weight).

The PET sample is characterized by  $[\eta] = 0.62 \text{ dl g}^{-1}$ , corresponding to a number average molecular weight  $M_n = 19\,600$ .

The isothermal crystallization experiments were performed in three different equipments: DSC (differential scanning calorimetry), HSLD (hot-stage microscopy equipped with a photodiode to measure light depolarization) and HSG (hot-stage microscopy equipped with a video system to measure growth rate).

Crystallizations in bulk were carried out under a nitrogen flux in a Perkin-Elmer DSC-7 instrument. The temperature scale was calibrated with high purity standards. PP samples (10 mg) were heated at  $10^{\circ}\text{C min}^{-1}$  to  $200^{\circ}\text{C}$ , kept at this temperature for 5 min, cooled at  $80^{\circ}\text{C min}^{-1}$  to the crystallization temperature and kept at  $T_c$  for the time necessary for crystallization. The  $T_c$  range varied from 120 to  $135^{\circ}\text{C}$ .

The PET specimens were heated at  $10^{\circ}\text{C min}^{-1}$  to  $300^{\circ}\text{C}$ , melted for 1 min, and cooled at  $100^{\circ}\text{C min}^{-1}$ . The  $T_c$  range varied from 190 to  $220^{\circ}\text{C}$ .

The equilibrium melting temperature  $T_m^{\circ}$  was evaluated by extrapolation of the melting temperature  $T_m$  with respect to the crystallization temperature  $T_c$ , according to

Hoffman and Weeks [2]. The  $T_m^{\circ}$  values thus obtained are: 457.5 K for PP sample A, 451.9 K for PP sample B, and 561 K for PET.

Light depolarization measurements were performed in an Orthoplan polarizing microscope, equipped with a Mettler FP52 heating device, coupled with a photo-sensitive diode in the eyepiece (HSLD). The evolution of crystallization was followed by continuous measurements of the light depolarization signal as a function of time. The light intensity detected by the diode before crystallization begins is zero. The relative crystallinity was calculated by dividing the light intensity after each time interval by the saturation value after a long time.

The number of nuclei per unit surface ( $N_s$ ) and growth rate ( $G$ ) measurements were carried out in a Leitz polarizing microscope (Labor Lux S), equipped with a Linkam TMHS 600 hot stage, camera and video camera (HSG). The numbers of nuclei were counted in photos taken at different times. The radii  $r$  of the spherulites were measured with a gridded system in a video. By plotting radius versus time, the growth rate was calculated by the slope of the straight lines obtained.

Thin films of PP (10–20  $\mu\text{m}$ ) were melted at 200°C for 5 min under nitrogen flux and cooled at 80°C  $\text{min}^{-1}$  to the selected  $T_c$ . The samples were kept at  $T_c$  for a time sufficient to crystallize fully. The PET specimens were submitted to the same thermal treatment, but the melting temperature was 283°C (limit of the hot stage).

### 3. Results and discussion

#### 3.1. Fold surface free energy determination from growth rate measurements

The growth rate  $G$  of spherulites or axialites during isothermal crystallization can be described, within a given regime, by the equation [1]

$$G = G_0 \exp[-U^*/R(T_c - T_x)] \exp[-K_g/T_c \Delta T f] \quad (2)$$

where  $G_0$  is a pre-exponential factor containing quantities not strongly dependent on temperature,  $U^*$  is a “universal” constant characteristic of the activation energy of chain motion (reptation) in the melt: its value is 6.28 kJ  $\text{mol}^{-1}$  [1].  $R$  is the gas constant,  $T_c$  the crystallization temperature;  $T_x$  represents the theoretical temperature below which all motion ceases; generally  $T_x \sim T_g - 30^\circ\text{C}$ .  $\Delta T = T_m^{\circ} - T_c$  is the undercooling;  $f$  is a correcting factor for variations in the heat of melting with temperature and is usually prescribed to be equal to  $2T_c/(T_c + T_m^{\circ})$ . The nucleation constant  $K_g$  is expressed by

$$K_{g\text{III}} = K_{g\text{I}} = 4 b_0 \sigma \sigma_e T_m^{\circ}/k \Delta H_m \quad (3)$$

in regimes III and I, and by

$$K_{g\text{II}} = 2 b_0 \sigma \sigma_e T_m^{\circ}/k \Delta H_m \quad (4)$$

in regime II;  $\sigma$  and  $\sigma_e$  are the lateral and fold surface free energies respectively,  $k$  is the Boltzmann constant and  $b_0$  the layer thickness.

The experimental measurements of growth rate  $G$  allow one to determine the nucleation constant from the slope of the plot of  $\ln G + U^*/R(T_c - T_x)$  versus  $1/T_c \Delta T f$ .

Clark and Hoffman [3] suggested a method of analysing the growth rate data in order to determine  $\sigma_c$  without knowing the heat of melting  $\Delta H_m$ . A value for  $\sigma$  is estimated by [1]

$$\sigma = \alpha \Delta H_m (a_o b_o)^{1/2} \quad (5)$$

where  $a_o$  is the width of the chain stem and  $\alpha$  is  $\simeq 0.1$ . The substitution of  $\sigma$  in Eqs. (3) and (4) yields

$$\sigma_c = K_{gIII} k / [4 b_o T_m^\infty \alpha (a_o b_o)^{1/2}] \quad (6)$$

or

$$\sigma_c = K_{gII} k / [2 b_o T_m^\infty \alpha (a_o b_o)^{1/2}] \quad (7)$$

Therefore the approximate value of  $\sigma$  makes it possible to determine the fold surface free energy value from growth rate measurements. This is the most direct method of estimating  $\sigma_c$  and has often been used by several authors [3–13].

### 3.2. $\sigma_c$ Determination by overall crystallization measurements

Eq. (2) can be applied to the overall crystallization process by replacing  $G$  with a suitable kinetic parameter. The application of Eq. (2) in the overall crystallization studies is supported by the fact that the kinetic data obtained from spherulitic growth and overall crystallization measurements yield identical values for the temperature at which a regime transition occurs. This result has been obtained for polyethylene and poly(ethylene oxide) fractions [14], for poly(1,3 dioxalane) [6, 15] and for isotactic polypropylene [16].

Thus, the temperature coefficient of the lamellar growth rate, which is involved in the transition, manifests itself in both overall crystallization and spherulitic growth.

Generally, the kinetic parameter used in Eq. (2) is the inverse of the semi-crystallization time ( $t_{1/2}$ ), i.e. the time necessary to reach 50% of the total crystallinity. In this case, Eq. (2) becomes

$$(1/t_{1/2}) = K' \exp[-U^*/R(T_c - T_\infty)] \exp[-K_g/T_c \Delta T f] \quad (8)$$

This approach is often found in the literature [15, 17–20], but it is obviously a simplified one, because it contains only one data point ( $t_{1/2}$ ) related to the overall crystallization process.

Another method of analysis, based on the Avrami equation [21] is presented below

$$X = 1 - \exp[-K(t - \tau)^n] \quad (9)$$

where  $X$  is the fraction crystallized at time  $(t - \tau)$ ,  $\tau$  is the induction period before crystallization begins and  $K$  is the crystallization constant. The Avrami plot,  $\ln[-\ln(1 - X)]$  versus  $\ln(t - \tau)$ , allows one to determine the coefficient  $n$  from the slope and  $\ln K$  from the intercept.

The Avrami intercept contains cumulative information about the whole crystallization curve at  $T_c$  and can supply quantitative kinetic information provided the crystallization mechanism is clear from the Avrami analyses.

In our case, the overall crystallization experiments performed in HSLD and DSC, on two samples of PP and one of PET, show an Avrami coefficient  $n$  equal to  $\sim 2$ . This result suggests heterogeneous nucleation from a fixed number of nuclei followed by bidimensional growth.

In fact, for experiments in HSLD on PP samples, the measurement of the nuclei number per unit surface ( $N_s$ ) shows that  $N_s$  does not vary with time; moreover, spherulitic growth is forced to occur in a bidimensional way, as the sample is a very thin film.

For DSC measurements, bulkier specimens than those for HSM study were used and, hence, volume nucleation could be more important. In this case, the number of nuclei per unit volume ( $N_v$ ) was determined for PP samples and was found constant during treatment time. Moreover, the  $n$  value of 2 can be justified assuming that DSC detects the evolution of heat from the growth of two-dimensional lamellae which constitute the spherulites. The determination of  $N_s$  and  $N_v$  for PET was not possible because of the very large number of nuclei.

In any case, the Avrami intercept can be written by the expression

$$\ln K = \ln(gNG^2) \quad (10)$$

where  $g$  is a geometrical factor,  $N$  can be  $N_s$  or  $N_v$  for HSLD and DSC measurements respectively, and  $G$  is the growth rate. Expression (10) can be written

$$\ln G = 0.5 \ln K - 0.5 \ln(gN) \quad (11)$$

By comparison with Eq. (1) in logarithmic form, it is possible to obtain [22]

$$0.5(\ln K) + U^*/R(T_c - T_x) = K'' - K_g/T_c \Delta T f \quad (12)$$

where  $K'' = (\ln gNG_0^2)/2$ .

In this way, as  $N$  does not vary with temperature, a plot of  $0.5(\ln K) + U^*/R(T_c - T_x)$  versus  $1/T_c \Delta T f$  is a straight line, whose slope yields the product of the surface energies.

We used this method of analysis, based on the Avrami equation, because we have verified that this expression, which is mathematically exact, describes polymer crystallization well in two and three dimensions (HSM and DSC), if there are no errors in the experimental procedure [23].

### 3.3. Determination of the induction time $\tau$

In order to use the Avrami equation, Eq. (9), it is necessary to know the induction time  $\tau$ , the time span before crystallization begins at  $T_c$ . This determination is not easy because, in general, instruments are not able to detect the first stages of crystallization (nucleation).

This is the reason why we can obtain different  $\tau$  values by varying the experimental technique, as reported in Table 1 for PP sample B.

The extrapolation of the spherulite radii to  $r = 0$  in the plot of  $r$  versus time allows one to know more exactly the  $\tau$  value at  $T_c$ . However, when HSLD and DSC are used, the start of crystallization is related to the sensitivity of the instrument: the values

Table 1

Induction time  $\tau$  values measured from isothermal crystallization experiments performed by DSC, by hot-stage microscopy equipped with a photodiode (HSLD) and by hot-stage microscopy equipped with a video system (HSG) on PP sample B

$T/^\circ\text{C}$	$\tau_{\text{DSC}}/\text{s}$	$\tau_{\text{HSLD}}/\text{s}$	$\tau_{\text{HSG}}/\text{s}$
120	17	-	$\approx 0$
123	22	6	$\approx 0$
125	29	21	$\approx 0$
128	30	51	$\approx 0$
130	46	69	$\approx 0$
132	87	137	$\approx 0$
135	196	900	$\approx 0$

obtained reflect the time needed before the instruments can detect any thermal or optical effect.

For example, for PP sample B the crystallization is fast at every  $T_c$  from 120 to 135°C: the measurements of radii suggest that nucleation occurs immediately when the sample reaches  $T_c$ . However, HSLD and DSC measure a crystallization process that begins at longer times.

It is interesting to observe that the Avrami plot for the overall crystallization measurements yields a straight line, as predicted by the theory, only when we use the corresponding experimental  $\tau$  value for each technique. If we use the "real"  $\tau$  value, more exactly measured from growth rate, in DSC data, we do not obtain a straight line. For example, Fig. 1 reports the Avrami plot for PP sample B crystallized in the DSC at  $T_c = 135^\circ\text{C}$ : the curve obtained by using a  $\tau$  value equal to 196 s, as calculated in DSC (see Table 1) is a perfect straight line. If  $\tau$  is 0, as calculated by extrapolation of spherulite radius to  $r = 0$ , the line is not straight up to 30% of relative crystallinity.

Because we believe that the Avrami theory is correct in describing the phenomenon that each instrument observes, we used the corresponding measured  $\tau$  value.

#### 3.4. Comparison between experimental and literature data

Table 2 reports the experimental and literature  $\sigma_c$  data obtained by different techniques (DSC, HSLD and HSG) and different methods of analysis for five polymers. For the overall crystallization experiments, two analytical methods (named the semi-crystallization time and the Avrami intercept method) are used, based on Eqs. (8) and (12). The growth rate data are analysed by Eq. (2).

For PET samples the measurement of growth rate was not possible because of the high number of nuclei and thus the small size of spherulites in the temperature range examined.

Literature data on PEEK [20, 24] and PP [16] are also reported: these are the only literature examples where measurements of  $\sigma_c$  by different experimental techniques (in

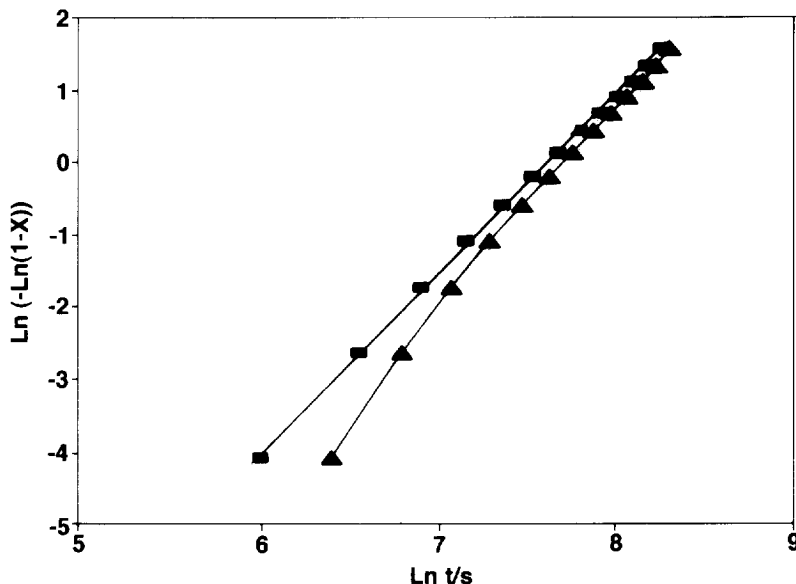


Fig. 1. Avrami plot for PP sample B crystallized in DSC at  $T_c = 135$  °C: ■,  $\tau = 196$  s, as obtained from DSC curve; ▲,  $\tau = 0$ , as obtained from HSG measurements.

Table 2

Fold surface free energy values calculated experimentally for PP-A, PP-B and PET and from literature for PEEK [20, 24] and PP [16]. The regimes at which the crystallization experiments are performed are indicated in Roman numerals

Equipment	Analytical method	$\sigma_e$ (erg cm <sup>-2</sup> )						
		PP-A	PP-B	PET	PEEK	PP		
		III	III	II	I	II	III	
DSC	$t_{1/2}$ <sup>c</sup>	92	77	151	121–170	160	187	178
DSC	Av. int. <sup>d</sup>	100	95	161	–	–	–	–
HSLD <sup>a</sup>	$t_{1/2}$	78	77	155	–	–	–	–
HSLD	Av. int	82	69	145	–	–	–	–
HSG <sup>b</sup>	$G$ <sup>e</sup>	50	54	–	41–101	138	146	150

<sup>a</sup> Hot-stage microscopy equipped with a photodiode that measures light depolarization. <sup>b</sup> Hot-stage microscopy equipped with a video system that allows the measurement of spherulitic growth. <sup>c</sup> Analysis method based on semi-crystallization time. <sup>d</sup> Analysis method based on Avrami intercept. <sup>e</sup> Analysis method based on growth rate.

these cases, DSC and HSG) are made and compared on the same sample. In this way, it is possible to be sure that the differences in  $\sigma_e$  values are due to the experimental techniques and not to some differences in the molecular characteristics of the polymer.

A good agreement between the  $\sigma_c$  values obtained for PP samples A and B, as well for PET, is observed by using DSC and HSLD and two different analytical methods (semi-crystallization time and Avrami intercept). In fact,  $\sigma_c$  varies between 80 and 100 erg cm<sup>-2</sup> for PP sample A, between 70 and 95 erg cm<sup>-2</sup> for PP sample B, and between 145 and 160 erg cm<sup>-2</sup> for PET. In this sense, the more correct method of analysis, the Avrami intercept method, yields similar results to the semi-crystallization time method. The growth rate data, instead, yield  $\sigma_c$  values that are lower than those obtained from the overall crystallization measurements. This difference is significant (about 30–50%). The same comparison for PET is not possible, because the growth rate was not measured.

Similar observations can be made using literature data. Janimak and Cheng [16] reported  $\sigma \cdot \sigma_c$  values for PP fractions obtained from linear crystal growth and overall crystallization data (DSC) in regimes I, II and III. In Table 2 the corresponding  $\sigma_c$  values, calculated assuming a value of 11.5 erg cm<sup>-2</sup> for  $\sigma$ , as indicated by the authors, are reported. The fold surface free energy value ranges between 160 and 187 erg cm<sup>-2</sup> from the overall crystallization data and between 138 and 150 erg cm<sup>-2</sup> from the growth rate data. This result corresponds to a difference of 14–28% between the two series of data.

The same observation can be made for the  $\sigma_c$  values obtained by Deslandes and coworkers [20, 24] on PEEK:  $\sigma_c$  varies between 121 and 170 erg cm<sup>-2</sup> from DSC data, and between 41 and 101 erg cm<sup>-2</sup> from HSG data.

In conclusion, the  $\sigma_c$  values obtained from overall crystallization measurements are always 15–50% higher than those obtained from growth rate data, when this comparison is made on the same sample. In order to explain this result it is necessary to remember that the overall crystallization data are much more complex and involve different phenomena, compared to the “simpler” growth rate data. However, in the Avrami analysis, all the secondary phenomena that can occur during the crystallization (thickening, exclusion of low molecular weight fractions, etc.) are left out: the straight line of the Avrami plot includes only the primary crystallization.

However, an experimental Avrami exponent of 2 has been explained by assuming that the growing lamellae cause the heat flow detected by DSC. The same phenomenon occurs when we measure the spherulite radius versus time.

Probably, the difference between the  $\sigma_c$  values reported in Table 2 are related to the fact that the analytical method based on growth rate data and on Eq. (1) is a more direct means to give a  $\sigma_c$  estimate.

Overall crystallization data require an analysis of the curves, obtained from DSC or from HSLD, by the Avrami equation or, more easily, by only one data point (the semi-crystallization time). This procedure is complicated by the difficulty in determining the induction time  $\tau$ , which depends on the sensitivity of the experimental technique used, as already mentioned. Thus it is possible to explain the difference between the results reported in Table 2.

#### 4. Conclusion

The problem in the determination of fold surface free energy by thermal analysis results from the difficulty in processing the experimental data. The overall crystalliza-



tion experiments performed by DSC or HSLD yield an isothermal crystallization curve which can be studied in two different ways: semi-crystallization time or the Avrami equation. Although the Avrami equation is more correct and complete, the two methods of analysis yield the same  $\sigma_c$  value.

Moreover it is to be noted that these  $\sigma_c$  values were 15–50% higher than those obtained from  $G$  measurements. This may be explained by the fact that the method of analysis based on  $G$  is more direct and does not require the approximations necessary for analysis of the overall crystallization data. This observation is important, because the different methods of determining  $\sigma_c$  by thermal analysis are used indiscriminately in the literature.

## References

- [1] J.D. Hoffman, G.T. Davis and J.I. Jr. Lauritzen, in N.B. Hannay (Ed.), *Treatise on Solid-State Chemistry*, Plenum Press, New York, 1976, Vol. 3, Chap. 7.
- [2] J.D. Hoffman and J.J. Weeks, *J. Res. Natl. Bur. Std. (A)*, 66 (1962) 13.
- [3] E.J. Clark and J.D. Hoffman, *Macromolecules*, 17 (1984) 878.
- [4] J.H. Magill, *J. Polym. Sci. A-2*, 5 (1967) 89.
- [5] J. Boon, G. Challa and D.W. van Krevelen, *J. Polym. Sci. A-2*, 6 (1968) 1791.
- [6] R. Alamo, J.G. Fatou and J. Guzman, *Polymer*, 23 (1982) 379.
- [7] R. Vasanthakumari and A.J. Pennings, *Polymer*, 24 (1983) 175.
- [8] P.J. Barham, A. Keller, E.L. Otun and P.A. Holmes, *J. Mater. Sci.*, 19 (1984) 2781.
- [9] B. Monasse and J.M. Haudin, *Colloid Polym. Sci.*, 263 (1985) 822.
- [10] B. Monasse and J.M. Haudin, *Colloid Polym. Sci.*, 266 (1985) 679.
- [11] D.B. Roitman, H. Marand, R.L. Miller and J.D. Hoffman, *J. Phys. Chem.*, 93 (1989) 6919.
- [12] S.Z.D. Cheng, J.J. Janimak, A. Zhang and H.N. Cheng, *Macromolecules*, 23 (1990) 298.
- [13] J.J. Janimak, S.Z.D. Cheng, P.A. Giusti and E.T. Hsieh, *Macromolecules*, 24 (1991) 2253.
- [14] R.C. Allen and L. Mandelkern, *Polym. Bull.*, 17 (1987) 473.
- [15] R. Alamo, J.G. Fatou and J. Guzman, *Polymer*, 23 (1982) 374.
- [16] J.J. Janimak and S.Z.D. Cheng, *Polym. Bull.*, 22 (1989) 95.
- [17] S. Lazcano, J.G. Fatou, C. Marco and A. Bello, *Polymer*, 29 (1988) 2076.
- [18] D.P. Heberer, S.Z.D. Cheng, J.S. Barley, S.H.-S. Lien, R.G. Bryant and F.W. Harris, *Macromolecules*, 24 (1991) 1890.
- [19] J.J. Janimak, S.Z.D. Cheng, A. Zhang and E.T. Hsieh, *Polymer*, 33 (1992) 728.
- [20] M. Day, Y. Deslandes, J. Roovers and T. Suprunchuk, *Polymer*, 32 (1991) 1258.
- [21] M.J. Avrami, *J. Chem. Phys.*, 7 (1939) 1103; 8 (1940) 212; 9 (1941) 177.
- [22] E.D. Zanotto, L. Zanotto and A. Celli, *Proc. 2nd Brazilian Congress on Polymers*, 2 (1993) 1112.
- [23] A. Celli and E.D. Zanotto, work in progress (1995).
- [24] Y. Deslandes, F.-N. Sabir and J. Roovers, *Polymer*, 32 (1991) 1267.